Size-dependent persistent photocurrent and surface band bending in *m*-axial GaN nanowires

Hsin-Yi Chen,[1,2,*] Reui-San Chen,[3] Nitin K. Rajan,[4] Fu-Chieh Chang,[5] Li-Chyong Chen,[1,†] Kuei-Hsien Chen,[1,3] Ying-Jay Yang,[5] and Mark A. Reed[4,2]

[1]*Center for Condensed Matter Sciences, National Taiwan University, Taipei 10617, Taiwan*
[2]*Yale University, Department of Electrical Engineering, New Haven, CT 06520, USA*
[3]*Institute of Atomic and Molecular Sciences, Academia Sinica, Taipei 10617, Taiwan*
[4]*Yale University, Department of Applied Physics, New Haven, CT 06520, USA*
[5]*Graduate Institute of Electronics Engineering, National Taiwan University, Taipei 10617, Taiwan*

(Received 14 December 2010; revised manuscript received 29 May 2011; published 21 November 2011)

The size-dependent persistent photocurrent (PPC), which refers to a photocurrent persisting for a long time after the excitation light source is terminated, has been investigated in *m*-axial GaN nanowires (NWs) with diameters of 20–130 nm. These NWs possess polar side surfaces and thus exhibit strong surface band bending (SBB). With different diameters, a different rise time in photoconductivity (PC) upon excitation light illumination and a different decay time in the PPC are observed; the latter is attributed to a long carrier lifetime caused by a frustrated recombination process. The intensity (I)-dependent photocurrent–gain (Γ) measurement displays a Γ-I dependence that follows a power-law relationship with fitting indices of ~0.85–0.89, indicating that the long carrier lifetime–induced PPC of GaN NWs is caused by an SBB effect instead of a bulk trap effect. In addition, size-dependent decay times reveal two regimes for the different sizes of NWs. The decay time of the NW above critical diameter (d_{crt}, 30–40 nm) is found to be ~13 000 s, while the smaller NW ($<d_{crt}$) is <800 s. Herein, we propose that the surface-induced effective barrier height for different sizes of GaN NWs is the dominant factor that explains the apparent size dependence. The temperature-dependent decay time measurements determine an effective barrier height of 226 meV for a 65-nm NW, whereas the 20-nm NW has an effective barrier height of 32 meV, confirming that SBB effects of different sizes are responsible for the size-dependent PPC in *m*-axial GaN NWs.

DOI: 10.1103/PhysRevB.84.205443 PACS number(s): 73.63.−b

I. INTRODUCTION

GaN nanowires (NWs) have attracted great interest in the past decade. Due to their wide direct band gap and unique geometry, the developments of optoelectronic nanodevices, e.g., light-emitting diodes,[1] photodetectors,[2,3] and diode lasers,[4] have been widely investigated. They also have been demonstrated as a promising building block in high electron mobility transistors,[5] biological sensors,[6,7] and solar cells.[8] These unique one-dimensional (1D) structures can change fundamental properties with regard to their corresponding bulk or thin film materials.[2,3] For instance, a GaN nanobridge (NB) device exhibited photoresponsivity two to three orders magnitude higher than bulk and thin film cases.[2] Therefore, the size effect could be an important factor, altering the fundamental transport property[9–11] and photoconductivity (PC).[2,3,11,12] For example, the size-confined 1D structure with a high surface-to-volume ratio can provide carriers with an anisotropic transport path. In addition to the electronic transport property and PC studied in GaN NWs, the persistent photocurrent (PPC), PC that can persist for a long time after the excitation light source has been shut off (thus retarding the recovery of the initial thermal equilibrium), is a fundamental property for GaN PC characterization. The PPC has been observed and reported in GaN thin film and bulk materials previously.[13–17] Many different methods have been utilized to investigate the origin of the PPC in GaN, e.g., photoluminescence,[13,14] optical absorption,[15] and PC.[16,18] Although the origin of the PPC has not been conclusively determined, the deep-level defects that act as recombination centers are generally considered possible causes of the PPC in GaN thin film or bulk materials.[14–17] However, investigations on the PPC in GaN NWs are sparse, and its origins are not clear. Herein, we investigate the first size-dependent PPC in *m*-axial GaN NWs. The purpose of this study is to identify the cause that gives rise to the PPC in GaN NW cases and verify how size affects the PPC behavior in GaN NWs.

II. THE PPC CHARACTERIZATION OF GaN NW

The PPC, due to frustrated carrier recombination in GaN NWs, is the most distinct characterization of PC compared to their and thin film counterparts. Figure 1(a) illustrates two photocurrent curves of a GaN NB device[2,3,19] (composed of an ensemble of GaN NWs, with an average diameter of 40 ± 20 nm and an average of 10 ± 2 μm, grown epitaxially between two GaN posts) and a nominally undoped GaN thin film with a thickness of 1 μm. The applied bias is 0.1 V in both cases, and the time interval is 0.5 s. Clearly, the GaN NB photocurrent persists for a long time, whereas the GaN thin film shows an evident direct recombination while the pumping light source was shut off. Figure 1(b) shows the typical PC response of a GaN NB device with an applied bias 0.1 V by illuminating an ultraviolet (UV)–light source at room temperature. As can be seen here, it takes <200 s for the current to be saturated. On the contrary, it takes >3000 s (~1 h) for measured current to recover its original dark current level. The result reveals that the rise time (τ_r) and decay time (τ_d) are not identical, which is significantly different from the conventional PC process. The different τ_r and τ_d in PC and the PPC process are generally attributed to the presence of a deep (bulk) trap effect in GaN thin film and

 ©2011 American Physical Society

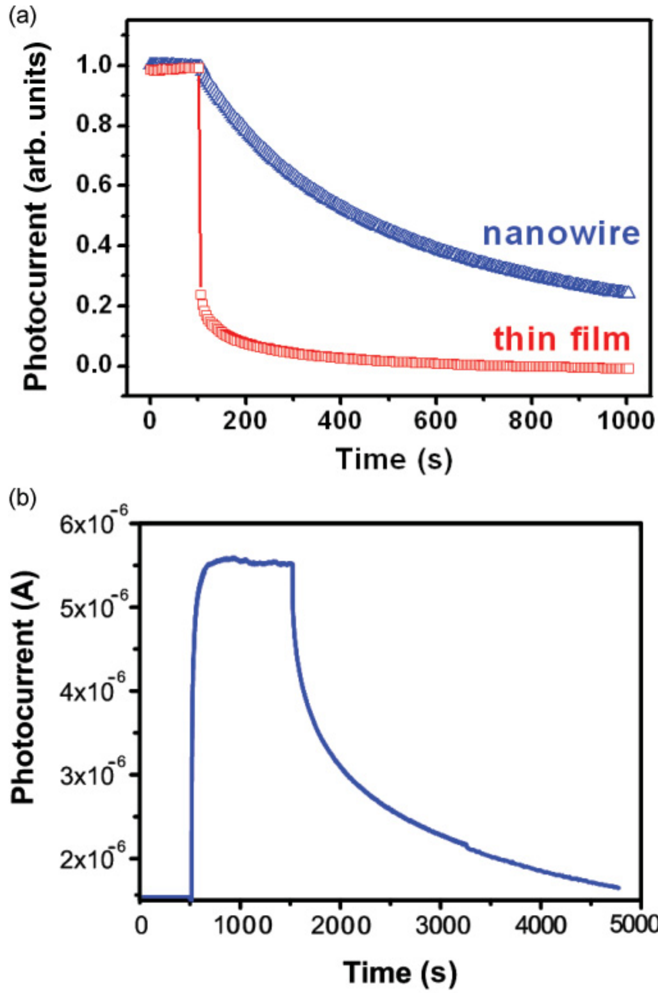

FIG. 1. (Color online) (a) The photocurrent curves of a GaN thin film (lower red line) and a GaN NB device (upper blue line) after turning off the UV-light source. The distinct difference between the two indicates less direct recombination in GaN NWs. (b) The photocurrent curve of GaN NBs under a DC bias of 0.1 V. The average diameter of a GaN NB is 40 ± 20 nm, and the average is 10 ± 2 μm.

bulk counterparts.[14–17] To gain further understanding of the PPC for the single GaN NW, we fabricated a single GaN NW device for the PPC measurements. The GaN NWs we utilized for single-NW measurements were grown via a vapor–liquid–solid mechanism in a catalytic chemical vapor deposition (CVD) system.[20] Typical lengths and diameters of GaN NWs are 5–20 μm and 20–130 nm, respectively. The structure of GaN NWs was verified by transmission electron microscopy to be single crystalline with a long axis in the $\langle 1\bar{1}0\rangle$ direction (*m*-axis).[3] The two-terminal single-NW devices were fabricated by electron-beam lithography (EBL).[21] A post treatment of rapid thermal annealing at 700 °C for 2 min was required to achieve the ohmic contact. The PC measurements of the single-NW samples were carried out on a two-probe station equipped with an optical microscope and two manipulators at room temperature. A semiconductor characterization system (Keithley model 4200-SCS) was utilized to source the direct current (DC) bias and measure the current. The light source for the PC measurements was provided by a He-Cd laser with a wavelength of 325 nm and a power of 0.5 mW.

III. CONTACT RESISTANCE ANALYSIS

Figure 2(a) displays the selected current-voltage curves of GaN NWs with three sizes. All curves show linear behavior, indicating a good ohmic contact condition in the fabricated single-NW devices. In addition to the qualitative analysis, the specific contact resistivity is quantitatively estimated by the transmission line method. The NW resistance and the associated contact resistance contribute to the total resistance, R_t, which is given by[22–24]

$$R_t = 2R_c + R_{\rm NW} = 2R_c + \frac{\rho_s}{\pi}\cdot\frac{l}{r^2}, \quad (1)$$

where R_c is the contact resistance, $R_{\rm NW}$ is the NW resistance, ρ_s is the sheet resistivity of the semiconductor, and l and r are wire length and radius, respectively.

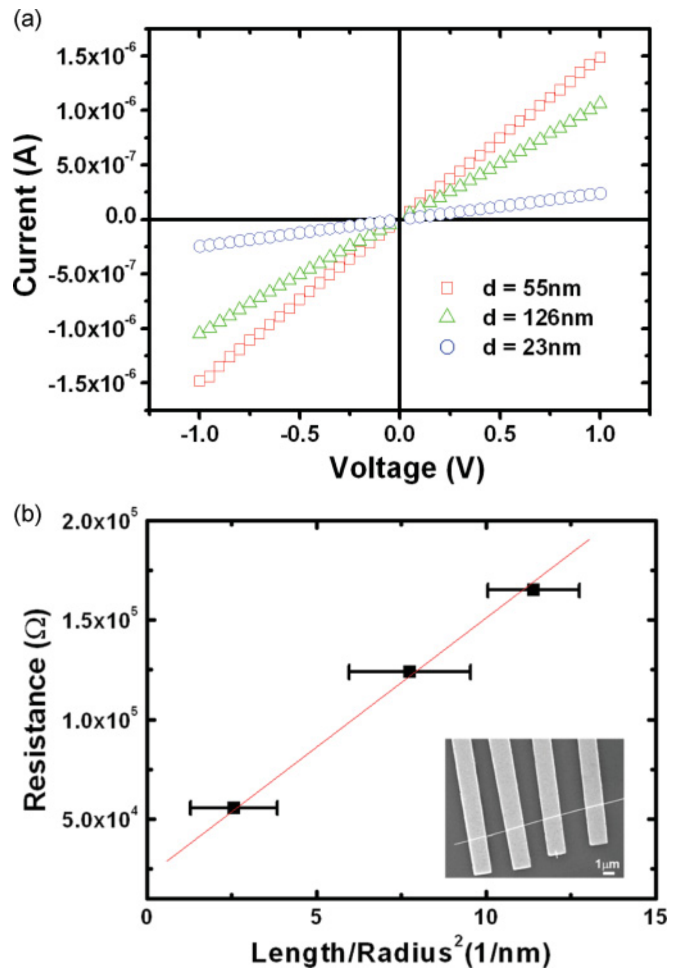

FIG. 2. (Color online) (a) Current-voltage curves with three diameters, indicating excellent ohmic contacts. (b) The plot of the total resistance (R_t) versus the length divided by the radius squared (l/r^2) of GaN NWs. The inset shows a typical field emission scanning electron microscopy image of a single-NW device of GaN with the Ti/Au (30/150 nm) metal contacts on the electrical insulating Si_3N_4/Si substrate. The length and diameter of the NW are 2–3 μm and 55 nm, respectively.

Figure 2(b) shows the R_t as a function of $\frac{l}{r^2}$ and an inset of a typical micrograph of a GaN NW device fabricated by EBL. The R_c can be evaluated as $\sim 1.3 \times 10^4$ Ω. The value of R_c is much smaller than the NW resistance ($R_{\mathrm{NW}} = 4.2 \times 10^4 - 1.5 \times 10^5$ Ω) so that we could ensure the measured resistance is primarily from the NW rather than the contact resistance. In addition, the calculated specific contact resistance (ρ_c) at 3.8×10^{-4} Ω-cm^2 is comparable to that given in previous reports.[23,25] The calculated resistance results confirm good contacts, allowing us to proceed to the PC measurements.

IV. THE PPC MECHANISMS OF GaN MATERIALS

A. Surface band bending and bulk trap effect

As mentioned before, the PPC means the photocurrent remains a long time after the light source has been shut off, implying a long carrier lifetime during the PC process. Generally, GaN NWs without intentional doping are always *n*-type;[21,26,27] thus, the photocurrent is predominantly determined by the lifetime of the minority hole. For the GaN materials, two probable long carrier lifetime mechanisms leading to the prolongation of the photohole lifetime have been investigated. First, the presence of hole traps in the *n*-type semiconductor could prolong the lifetime of the excess electron and contribute to a long carrier lifetime in GaN films.[28–30] Second, a mechanism different from the minority bulk trap mechanism proposed by Calarco *et al.*,[12] Queisser and Theodorou,[31] and Munoz and colleagues[32,33] originated from a significant surface energy band bending in GaN, which would localize the excess carrier distribution. The very slow recombination of the hole, either with a spatially separated free electron or via the trapped electron at the surface, prolongs the carrier lifetime. Thus, the surface-induced carrier localization is proposed to be one of the main causes of the long carrier lifetime. Consequently, the 1D nanostructure with a high surface-to-volume ratio could make the behavior of carrier localization more significant and thus dominate the PPC process. However, hole traps cannot be neglected in GaN and could govern the long carrier lifetime mechanism, whether the form is film or NW. Stevens *et al.*[28] and Binet *et al.*[29] have explained that the contribution of a trap in the GaN films can be identified by the intensity-dependent behavior of the gain (Γ) measurement. The definition of the physical parameter of Γ is characterized and described as follows.

B. The definition and calculation of PC parameters

In principle, photoconduction is composed of two processes: optical absorption and electronic transport. To understand the contribution of electronic transport during the PC process, the optical absorption of GaN NWs needs to be defined first. The efficiency (η) of photon absorption to create electron–hole pairs (EHPs) is dominated by the quantum efficiency $\eta_q = 1 - e^{-\alpha d}$, where α is the absorption coefficient and d is the wire diameter. Taking into account the normal-incidence reflection loss, the net efficiency can be written as $\eta = (1 - R_o)(1 - e^{-\alpha d})$, where R_o is the optical reflectivity. Both R_o and α are wavelength dependent, and they are estimated to be $R_o \sim 20\%$ and $\alpha \sim 10^5$ cm^{-1} at a wavelength of 325 nm.[34] The estimated η of all samples is in the range of 14%–57%. From the values of η and the photocurrent Δi, the gain Γ, a factor determining the efficiency of electron transport and carrier collection during the PC process, can be deduced from Razeghi and Rogalski's equation[35]

$$\Gamma = \frac{E \times \Delta i}{e \times \eta \times P}, \tag{2}$$

where E is the photon energy at 3.81 eV and e is electron charge. The effective absorbed power P can be calculated as

$$P = I \cdot A = I \cdot d \cdot l, \tag{3}$$

where I is the intensity of the incident light and A is the product of the diameter and length of a NW, i.e., the projecting area of a single wire.

C. The PPC origin of GaN NW

By the definition and calculation of Eq. (2), we are able to obtain Γ values versus NW diameters. For the GaN PC cases, under the low-level excitation below a critical intensity (usually the power density I <40 W/m^2), most excess holes are captured by the traps and the hole traps govern the gain and make it independent of the intensity, i.e., Γ = const. Once the critical intensity is exceeded, the hole traps are filled by the photocarriers and the intrinsic recombination occurs, making the relationship between Γ and I follow a power law, i.e., $\Gamma \propto I^{-k}$, where $k = 0.5$. On the other hand, the fitting index is ∼0.8–0.9 if the PPC mechanism is caused by surface band bending (SBB). Based on this understanding, the intensity-dependent Γ versus I measurements of the GaN single NW have been performed to investigate the mechanism for bringing out the PPC in the different sizes of GaN NWs. Complementary to the observation of the size dependence of dark conductivity and PC measurements, the size effects are enhanced when the NW size is decreased, allowing a critical diameter (d_{crt}) of ∼30–40 nm to be identified.[11] Hence, we selected three diameters above and below the d_{crt} of 30–40 nm. Figure 3 illustrates the Γ versus I measurement with the three selected diameters of 20, 65, and 130 nm. We observed that all $\Gamma - I$ curves show a clear power law ($\Gamma \propto I^{-0.9}$) in the intensity range over two decades from 0.7 to 100 W/m^2. In addition, the fitting indices of 20-, 65-,

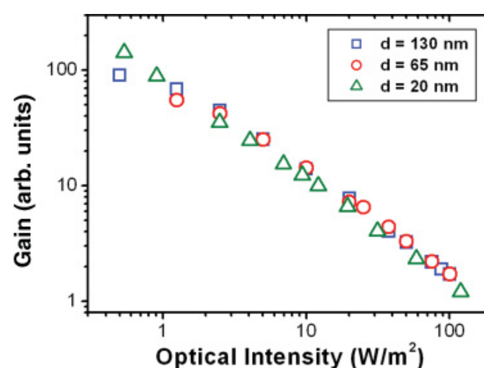

FIG. 3. (Color online) Power-dependent photocurrent–gain measurements for the GaN NWs with diameters of 20, 65, and 130 nm. The fitting indices of three curves are between 0.85 and 0.89, implying the dominant mechanism for the PPC of GaN NWs is SBB.

and 130-nm NWs are 0.87, 0.89, and 0.85, respectively. All fitting indices are found to be ∼0.8–0.9, which represents that the PC mechanism of GaN NWs is dominant by SBB other than the bulk trap effect, which should have an index value of 0.5.[28,29] This result also strongly suggests the photocarrier lifetimes are determined by the intrinsic recombination rather than the extrinsic recombination originated from the existence of the hole trap.[28,29] Moreover, the Γ-*I* dependence with the fitting *k* value of ∼0.9 is consistent with the results of Munoz and colleagues.[32,33] The agreement further suggests the GaN NW has a similar surface-dominant photocurrent mechanism as the undoped GaN films, and it suggests the long carrier lifetime enhancement is due to this high surface-to-volume ratio of the 1D structure.

V. SIZE-DEPENDENT RISE/DECAY TIME AND BAND DIAGRAMS

If the PPC is actually caused by an SBB-induced long carrier lifetime, intensity-dependent measurements (as shown in Fig. 3) should have a characteristic gain–intensity dependence. Upon UV-light illumination, generated EHPs suppress the band bending of GaN NW. On the other hand, after the UV light is turned off, the SBB recovers to the thermal equilibrium status and EHPs are spatially separated by the SBB, prolonging the recombination lifetime. Since SBB is flattened while the light source is illuminating, a τ_d measurement might be more adequate than a τ_r measurement for the investigation of the PPC. Therefore, to quantify the PC τ_r and τ_d, the transient curves are normalized and displayed in Fig. 4(a) and its inset, respectively. The curves were recorded after the light source at room temperature was shut off. The quantitative analysis of the photocurrent as a function of time follows the general stretched exponential model, used for materials affected by a nonexponential nature of the photocurrent decay.[36] According to this model, the photocurrent decay curve could be described by the equation

$$\Delta I(t) = \Delta I_0 \exp[-(t/\tau_d)^{\beta}], \qquad (4)$$

where $\Delta I(t) = I(t) - I(d)$ and $\Delta I_0 = I(0) - I(d)$, $I(t)$ is the current value at time t after the light is terminated, $I(d)$ is the current measured while the sample is in the dark, and $I(0)$ is the saturated current value after the light source is pumped for a period. The index value of β means the stretching exponential, and again, τ_d is the decay time.

Figure 4(a) displays the photocurrent decay curves of two sizes of GaN NWs with diameters 20 and 65 nm. The solid (red) lines are fitting lines for two curves from Eq. (4). By the definition of Eq. (4), the τ_d and β of these two NWs can be calculated. The evaluating τ_d of a 65-nm NW is >13 000 s, whereas the τ_d of the 20-nm NW is <800 s. The stretching exponential β is also calculated to be 0.46 and 0.79 for the 65- and 20-nm GaN NW, respectively. As can be seen here, the obvious τ_d differences (>10 times) show a significant size effect in GaN NWs when the diameter is smaller than the $d_{\rm crt}$ of 30–40 nm, coinciding with previous work for *m*-axial GaN NWs.[11] Furthermore, because the PPC of the *m*-axial GaN NWs is dominated by SBB from the intensity-dependent photocurrent–gain measurement, as shown in Fig. 3 (i.e., longer carrier lifetime indicates stronger band bending), the

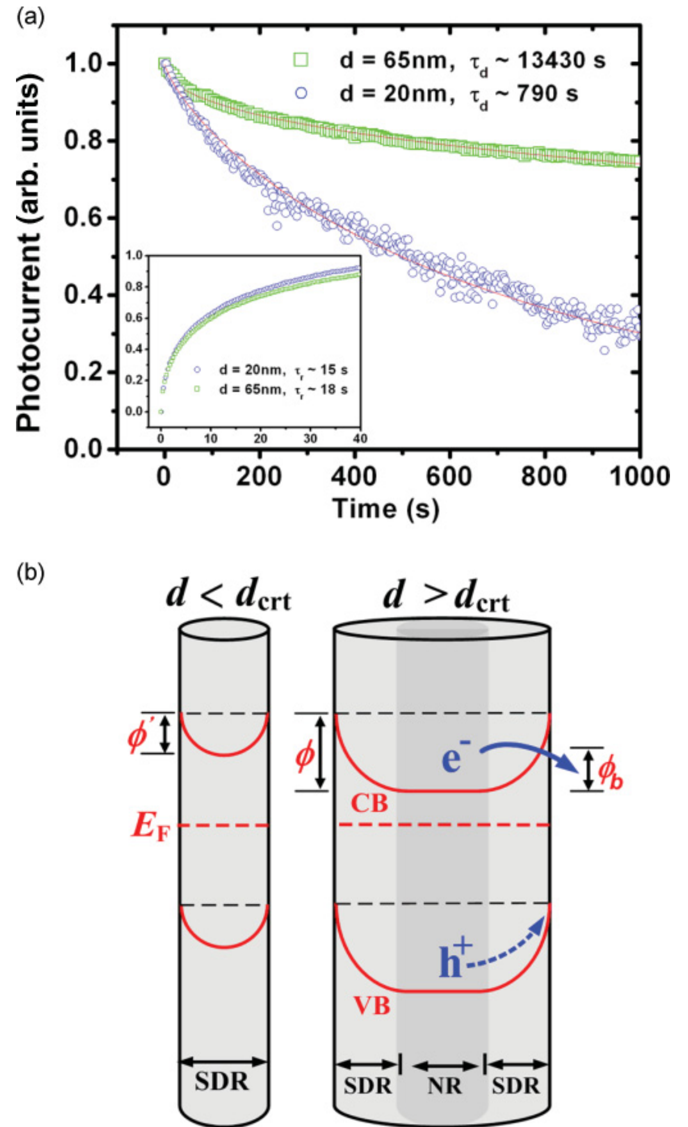

FIG. 4. (Color online) (a) The normalized photocurrent curves after and before (inset) the pumping light source is shut off for individual GaN NWs with diameters of 65 and 20 nm. (b) The schematic of real-space energy band diagrams for the GaN NWs with different diameters, where E_F is the Fermi level, CB is the conduction band, VB is the valence band, e^- is the electron, h^+ is the hole, NR is the neutral region, and SDR is the surface depletion region.

strong size-dependent τ_d results could be explained by the real-space band diagrams shown in Fig. 4(b). For NWs > $d_{\rm crt}$, there is a neutral region inside the NW and stronger band bending. As the NW diameter goes <$d_{\rm crt}$, the neutral region disappears and the barrier responsible for the SBB decreases, causing a substantially shortened carrier lifetime. This explains the >10-times decrease of τ_d as the NW diameter decreases <$d_{\rm crt}$. However, the obvious size dependence cannot be obtained from the size-dependent τ_r measurement, shown as the inset of Fig. 4. The same samples were measured in the τ_r experiment. The evaluated τ_r from the inset is 15 and 18 s for the 20-nm (blue circles) and 65-nm (green squares) GaN NW, respectively. The τ_r for the 20-nm NW indicates a slightly

weaker SBB compared to that of the 65-nm NW. However, the difference is much less than the τ_d results previously discussed. It may also imply that the SBB is flattened under UV-light illumination so that the τ_r result does not reveal distinct difference (>10 times) obtained in the τ_d measurement. As illustrated in Fig. 3, we could observe that both GaN NWs with diameters of 20 and 65 nm show indices of ∼0.9. Even for the 20-nm NW, smaller than the d_{crt} of 30–40 nm, PC is still dominated by SBB but does not exhibit a smaller fitting index value. It is because the "degree" of SBB cannot be distinguished from the index under the same PC mechanism (i.e., under PC dominated by SBB, or $k \approx 0.8$–0.9, the index of 0.89 does not indicate stronger bending than that of the index of 0.83.) We can only conclude that indices between 0.8 and 0.9 verify a long carrier lifetime mechanism induced by SBB. Size-dependent τ_d measurements are more convincing for identifying the "degree" of SBB in GaN NWs.

VI. EFFECTIVE BARRIER HEIGHT OF GaN NW

Since SBB is responsible for the PPC in GaN NWs, and the maximal barrier height of SBB (ϕ) for different sizes of GaN NWs is the major cause of the size-dependent PPC, the measurement of ϕ for GaN NWs is thus critical. In general, there are some methods to measure the surface potential or barrier height of films, e.g., the x-ray photoemission spectroscopy[37,38] (XPS) technique and the electrostatic (electric) force microscopy[39,40] (EFM) method. In this study, we provide another method to evaluate the "effective" barrier height, which is directly derived from the PPC results. By combining the qualitative analysis of Eqs. (4) and (5) as formulated here, the effective barrier height could be evaluated by

$$\tau_d = A \exp(-\phi_b/kT), \tag{5}$$

where A is a constant, ϕ_b is the "effective" barrier height, k is the Boltzmann constant of 8.62×10^5 (eV/K), and T is a temperature (K).

Figure 5(a) illustrates the temperature-dependent photocurrent curves for a single GaN NW of 65 nm after the pumping light source is terminated. The measurement was operated in vacuum with am applied bias of 1 V from 80 to 300 K. By utilizing Eq. (4), the fitted τ_d is found to increase with decreasing temperature. This implies that SBB is stronger at a low temperature, thus prolonging the carrier lifetime and leading to a longer τ_d. Figure 5(b) plots the relationship of τ_d to T for the selected GaN NWs of 65 nm (solid black circle) and 20 nm (solid red square). The τ_d for a 65-nm GaN NW is significantly longer than that of the 20-nm counterpart at the same temperature. The τ_d at low temperature (<100 K) did not change obviously, unlike the case at high temperature. This can be attributed to the much reduced thermal activation mechanism occurring at low temperature, leading to the little change of τ_d compared to that in the high temperature region.[41] Therefore, by evaluating ϕ_b at high temperature (150–300 K) from Fig. 5(b), the 65-nm NW shows the fitting ϕ_b of 226 meV, while the 20-nm NW is 32 meV. The seven-times difference implies that a NW $<d_{crt}$ possesses weaker band bending. A similar size dependence is found for the τ_d result, as previously discussed, i.e., the SBB is weaker when the diameter goes $<d_{crt}$. This is consistent with the SBB approach, since $>d_{crt}$, the n-type NWs have a bigger volume to supply sufficient surface-trapped electrons, which induces strong SBB and ϕ due to the negatively charged surface states. Once NWs go $<d_{crt}$, the smaller volume of NWs would provide less surface charge, leading to lower ϕ_b and shorter τ_d [Fig. 5(b)]. The sharp decrease of τ_d below a critical size can also be realized by the decrease of ϕ_b. Our fitting ϕ_b is lower than the reported value of 0.5–0.6 (GaN thin film) measured by XPS.[37] The probable reason is that ϕ measured by XPS or EFM indicates the difference between the bottom of the conduction band and the valence band maximum, i.e., photoelectrons should overcome ϕ to recombine with the photoholes at the surface. However, for the NWs, photoelectrons might be capable of going through a lower ϕ and may recombine with the photoholes at the surface, as illustrated in Fig. 4(b). This can elucidate why the derived ϕ_b is lower than the value of thin films.

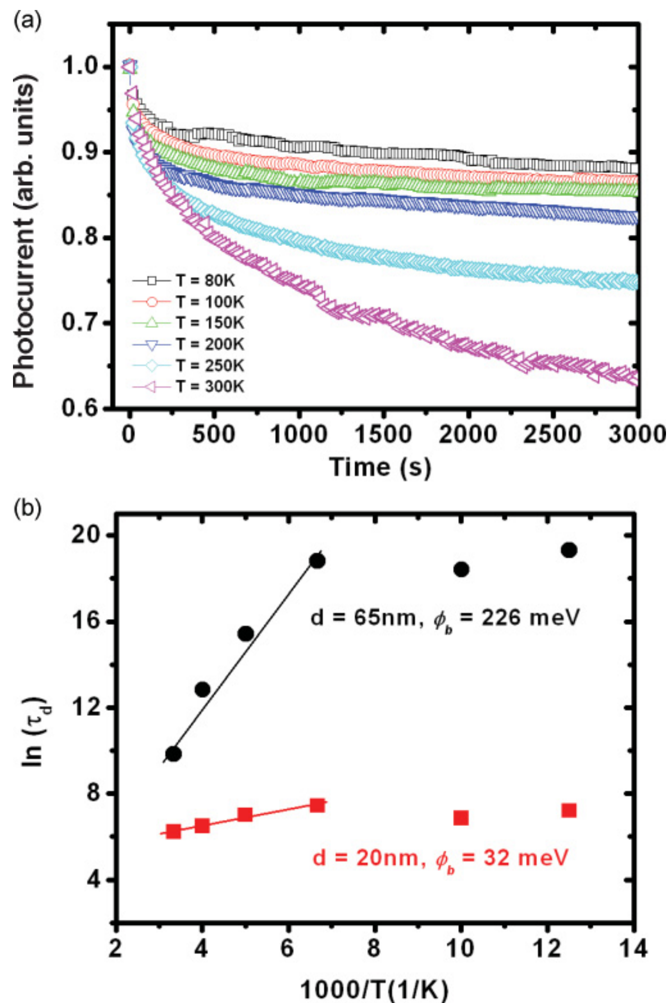

FIG. 5. (Color online) (a) The temperature-dependent photocurrent curves of an individual GaN NW with a diameter of 65 nm. All curves measured under different temperatures are monitored after turning off the UV-light source. (b) The plot of $\ln(\tau_d)$ versus $1000/T$ illustrates the fitting ϕ_b of two different NWs with the diameter 65 nm (solid black circles) and 23 nm (solid red squares).

VII. SURFACE POLARITY IN GaN NWs

In addition, the different crystallographic orientation (surface polarity) might play an important role in causing the SBB and the PPC in *m*-axial GaN NWs. As the *c*-plane GaN is a polar surface, which is different from the nonpolar *m*- and *a*-planes, the CVD NWs with *m*-axial growth orientation expose *c*-plane side walls, thus exhibit strong surface polarity. On the contrary, the *c*-axial NWs grown by molecular beam epitaxy have no surface polarity on their side walls. The polar surface of GaN has been reported as revealing higher surface activity to the adsorption of ambient molecules, e.g., oxygen.[42,43] Chen *et al.* also revealed that oxygen plays a major role in leading to the strong SBB at the surface of *m*-axial GaN NWs.[44] Furthermore, we found the origin of the PPC of *m*-axial GaN NWs was ascribed to SBB obtained by an intensity-dependent photocurrent–gain result. Therefore, the direct correlation between stronger polarity and higher band bending of the surface was thus obtained in this research.

VIII. CONCLUSION

In conclusion, the size-dependent PPC of *m*-axial GaN NWs grown by a CVD approach has been investigated in this study. The inherent "polarity" of the side surfaces of the *m*-axial GaN NWs leads to a strong SBB, and the origin of the PPC of *m*-axial GaN NWs is ascribed to this SBB instead of a bulk trap effect, which is further verified by an intensity-dependent photocurrent–gain measurement ($k \approx 0.9$). The different τ_r in PC and τ_d observed in the PPC is due to the suppressed SBB under illumination. We have identified the τ_d measurement, instead of the τ_r measurement, as a method for identifying the "degree" of SBB. Furthermore, the derived ϕ_b of the GaN NW $<d_{\rm crt}$ is much lower ($\sim$32 meV) than the values ($\sim$226 meV) of NW $> d_{\rm crt}$, confirming that weaker band bending exists in smaller GaN NWs. This study provides strong evidence of a surface-dominant transport property in GaN NWs due to the presence of surface depletion and band bending. Understanding of the surface-induced size effect on the PPC and electronic transport could expedite the new-generation design and application of optoelectronic devices by utilizing GaN NWs.

ACKNOWLEDGMENTS

This research was financially supported by Ministry of Education and National Science Council in Taiwan. Technical support from Academia Sinica Research Project on Nano Science and Technology is gratefully acknowledged.

[*]d95943019@ntu.edu.tw
[†]chenlc@ntu.edu.tw
[1]F. Qian, S. Gradecak, Y. Li, C. Y. Wen, and C. M. Lieber, Nano. Lett. **5**, 2287 (2005).
[2]R. S. Chen, H. Y. Chen, C. Y. Lu, K. H. Chen, C. P. Chen, L. C. Chen, and Y. J. Yang, Appl. Phys. Lett. **91**, 223106 (2007).
[3]R. S. Chen, S. W. Wang, Z. H. Lan, J. T. H. Tsai, C. T. Wu, L. C. Chen, K. H. Chen, Y. S. Huang, and C. C. Chen, Small **4**, 925 (2008).
[4]M. H. Huang, S. Mao, H. Feick, H. Yan, Y. Fang, Y. Wu, H. Kind, E. Weber, R. Russo, and P. Yang, Science **292**, 1897 (2001).
[5]Y. Li, J. Xiang, F. Qian, S. Gradecak, Y. Fang, Y. Wu, H. Yan, D. A. Blom, and C. M. Lieber, Nano. Lett. **6**, 1468 (2006).
[6]C. P. Chen, A. Gangurly, C. H. Wang, C. W. Hsu, S. Chattopadhyay, Y. K. Hsu, Y. C. Chang, K. H. Chen, and L. C. Chen, Anal. Chem. **81**, 36 (2009).
[7]Y.-T. Lai, A. Ganguly, L.-C. Chen, and K.-H. Chen, Biosens. Bioelectron. **26**, 1688 (2010).
[8]Y. J. Dong, B. Z. Tian, T. J. Kempa, and C. M. Lieber, Nano. Lett. **6**, 1468 (2006).
[9]M. Niebelschutz, V. Cimalla, O. Ambacher, T. Machleidt, J. Ristic, and E. Calleja, Phys. E **37**, 200 (2007).
[10]B. S. Simpkins, M. A. Mastro, C. R. Eddy Jr., and P. E. Pehrsson, J. Appl. Phys. **103**, 104313 (2008).
[11]H. Y. Chen, R. S. Chen, F. C. Chang, L. C. Chen, K. H. Chen, and Y. J. Yang, Appl. Phys. Lett. **95**, 143123 (2009).
[12]R. Calarco, M. Marso, T. Richter, A. I. Aykanat, R. Meijers, A. V. D. Hart, T. Stoica, and H. Luth, Nano. Lett. **5**, 981 (2005).
[13]H. M. Chen, Y. F. Chen, M. C. Lee, and M. S. Fang, J. Appl. Phys. **82**, 899 (1997).
[14]C. V. Reddy, K. Balakrishan, H. Okumura, and S. Yoshida, Appl. Phys. Lett. **73**, 244 (1998).
[15]S. J. Chung, M. S. Jeong, O. H. Cha, C. H. Hong, E. K. Suh, H. J. Lee, Y. S. Kim, and B. H. Kim, Appl. Phys. Lett. **76**, 1021 (2000).
[16]C. H. Qiu, C. Hoggatt, W. Melton, M. W. Leksono, and J. I. Pankove, Appl. Phys. Lett. **66**, 2717 (1995).
[17]C. Johnson, J. Y. Lin, H. X. Jiang, M. Asif Khan, and C. J. Sun, Appl. Phys. Lett. **68**, 1808 (1996).
[18]J. Xu, D. Yu, Y. Tang, Y. Kang, X. Li, X. Li, and H. Gong, Appl. Phys. Lett. **88**, 072106 (2006).
[19]See Supplemental Material at http://link.aps.org/supplemental/10.1103/PhysRevB.84.205443 for the characterization of GaN NB device.
[20]C. C. Chen, C. C. Yeh, C. H. Chen, M. Y. Yu, H. L. Liu, J. J. Wu, K. H. Chen, L. C. Chen, J. Y. Peng, and Y. F. Chen, J. Am. Chem. Soc. **123**, 2791 (2001).
[21]E. Stern, G. Cheng, E. Cimpoiasu, R. Klie, S. Guthrie, J. Klemic, I. Kretzschmar, E. Steinlauf, D. Turner-Evans, E. Broomfield, J. Hyland, R. Koudelka, T. Boone, M. Young, A. Sanders, R. Munden, T. Lee, D. Routenberg, and M. A. Reed, Nanotechnology **16**, 2941 (2005).
[22]D. K. Schroder, *Semiconductor Material and Device Characterization* (Wiley, New York, 1990).
[23]M. H. Ham, J. H. Choi, W. Hwang, C. Park, W. Y. Lee, and J. M. Myoung, Nanotechnology **17**, 2203 (2006).
[24]C. Y. Chang, G. C. Chi, W. M. Wang, L. C. Chen, K. H. Chen, F. Ren, and S. J. Pearton, Appl. Phys. Lett. **87**, Art. No. 093112 (2005).
[25]E. Stern, G. Cheng, M. P. Young, and M. A. Reed, Appl. Phys. Lett. **88**, 053106 (2006).

[26]T. Kuykendall, P. Pauzauskie, S. Lee, Y. Zhang, J. Goldberger, and P. Yang, Nano. Lett. **3**, 1063 (2003).
[27]Y. Huang, X. Duan, Y. Cui, and C. M. Lieber, Nano. Lett. **2**, 101 (2002).
[28]K. S. Stevens, M. Kinniburgh, and R. Beresford, Appl. Phys. Lett. **66**, 3518 (1995).
[29]F. Binet, J. Y. Duboz, E. Rosencher, F. Scholz, and V. Harle, Appl. Phys. Lett. **69**, 1202 (1996).
[30]R. H. Bube, *Photoelectronic Properties of Semiconductors* (Cambridge, New York, 1992).
[31]H. J. Queisser and D. E. Theodorou, Phys. Rev. Lett. **43**, 401 (1979).
[32]E. Munoz, E. Monroy, J. A. Garrido, I. Izpura, F. J. Sanchez, M. A. Sanchez-Garcia, B. Beaumont, and P. Gibart, Appl. Phys. Lett. **71**, 870 (1997).
[33]J. A. Garrido, E. Monroy, I. Izpura, and E. Munoz, Semicond. Sci. Technol. **13**, 563 (1998).
[34]T. Kawashima, H. Yoshikawa, S. Adachi, S. Fuke, and K. Ohtsuka, J. Appl. Phys. **82**, 3528 (1997).
[35]M. Razeghi and A. Rogalski, J. Appl. Phys. **79**, 7433 (1996).
[36]C. H. Qiu and J. I. Pankove, Appl. Phys. Lett. **70**, 1983 (1997).
[37]M. Kocan, A. Rizzi, H. Luth, S. Keller, and U. K. Mishra, Phys. Status Solid. B **234**, 773 (2002).
[38]J. P. Long and V. M. Bermudez, Phys. Rev. B **66**, 121308 (2002).
[39]P. Girard, Nanotechnology **12**, 485 (2001).
[40]Y. T. Lin, W. S. Su, W. S. Su, and Y. F. Chen, Solid State Commun. **130**, 49 (2004)
[41]Y. T. Lin, H. C. Yang, and Y. F. Chen, J. Appl. Phys. **87**, 340 (2000).
[42]T. K. Zywietz, J. Neugebauer, and M. Scheffler, Appl. Phys. Lett. **74**, 1695 (1999).
[43]M. Sumiya, K. Yoshimura, K. Ohtsuka, and S. Fuke, Appl. Phys. Lett. **76**, 2098 (2000).
[44]R. S. Chen, C. Y. Lu, K. H. Chen, and L. C. Chen, Appl. Phys. Lett. **95**, 233119 (2009).